ESAIM: M2AN 52 (2018) 2409–2431
https://doi.org/10.1051/m2an/2018065

ESAIM: Mathematical Modelling and Numerical Analysis
www.esaim-m2an.org

SIMULATION AND STRUCTURAL OPTIMIZATION OF 3D TIMOSHENKO BEAM NETWORKS BASED ON FULLY ANALYTIC NETWORK SOLUTIONS

Tobias Kufner[1], Günter Leugering[1], Johannes Semmler[1], Michael Stingl[2,*] and Christoph Strohmeyer[1]

Abstract. This article is concerned with the efficient and accurate simulation and optimization of linear Timoshenko beam networks subjected to external loads. A solution scheme based on analytic ansatz-functions known to provide analytic solutions for the deformation and rotation of a single beam with given boundary data is extended to the full network. It is demonstrated that the analytic approach is equivalent to a finite element (FE) method where only one element with a suitably chosen shape function per beam is required. The solution of the FE-type system provides analytic solutions at the nodes, from which the solutions along the beams can be reconstructed. Consequently analytic solutions for the network can be computed by a numerical scheme without applying a spacial discretization. While the assembly of the local stiffness matrices is slightly more expensive compared to an FE model using, *e.g.*, linear ansatz-functions, the complexity of the solution of the FE-system is not. This is particularly interesting for topology and material optimization problems formulated on the network. In order to demonstrate the efficiency of the approach a numerical comparison to the case of linear ansatz-functions is provided followed by a series of studies with topology and multi-material optimization problems on networks.

Mathematics Subject Classification. 34B45, 68U20, 74P05, 90C30, 90C90.

Received June 22, 2017. Accepted October 28, 2018.

1. Introduction

Numerous structures in engineering and architecture can be modeled as space frames. Examples include bridges, roof support structures and aircraft or car frames. The first problem to consider is the structural analysis of such a frame, either analytically or via numerical methods such as the finite element method. There are several methods available to model the actual struts and joints of such a structure (depending on the desired application), each of which also affect the simulation effort. Moreover, on the basis of a given frame model, various structural optimization problems can be posed. The vast majority of these can be grouped into

Keywords and phrases. Timoshenko beam network, analytic solutions, topology optimization, multi-material optimization.

[1] Friedrich-Alexander-Universität Erlangen-Nürnberg (FAU), Department of Mathematics, Applied Mathematics 2, Cauerstraße 11, 91058 Erlangen, Germany.

[2] Friedrich-Alexander-Universität Erlangen-Nürnberg (FAU), Department of Mathematics, Mathematical Optimization, Nägelsbachstraße 49b, 91052 Erlangen, Germany.

*Corresponding author: michael.stingl@fau.de

four broad categories: sizing optimization, topology optimization, (multi-)material optimization and geometry or shape optimization.

One of the most common physical models in structural optimization is the pin-jointed truss, which consists of bars that can transmit axial forces only. Truss topology optimization has been an active research field for many years with contributions from *e.g.* [1, 2, 4, 11], [16] or [26]. Alternatively, the frame can be constructed from beam elements. Taking transport of momentum and bending of these elements into account results in the well-known Euler-Bernoulli beam theory. However, for some applications, shear deformation in the beam elements may not be negligible. In this case the Timoshenko beam theory is more appropriate. Some examples for structural optimization with beam networks exist. Fredricson *et al.* [8] demonstrate topology optimization for frame structures with Euler-Bernoulli beams and additional modeling of flexible joints, while [7] discusses an optimal material selection. In [36, 37] beams are used to model whole product families of car frames. The authors suggest a design process based on simultaneous size, shape and topology optimization. In contrast to our approach no analytic beam solutions are utilized. There are even commercial implementations of structural optimization solvers applied to frame structures, however the computational complexity of the resulting problems is typically one order of magnitude higher compared to truss topology design problems as a spacial discretization of the individual beams is necessary in order to obtain solutions which are sufficiently accurate.

In this article, we use networks of linear Timoshenko beam elements with rigid joints [17] as a basis for our simulation model. As already mentioned previously our major goal is to develop an analytic solution scheme for the whole Timoshenko network problem, as a consequence of which no discretization along individual beams is required. The analytic solution scheme is based on so called analytic ansatz-functions for individual Timoshenko beams. Accordingly, below we provide a short review of Timoshenko beam models and related ansatz-functions.

The Timoshenko beam, first derived by Timoshenko, see [34,35], is a widely-used model within solid mechanics. For the numerical analysis of such a simulation model, typically a finite element approach is used. Early examples include [15], in which a cubic function for the bending deformation is used. Thomas *et al.* [32] gives an overview of several 2D Timoshenko beam elements. In [33] an element with nodal degrees of freedom and cubic polynomials for displacement and rotation is presented, as well as comparisons to the application of alternative elements used in the literature. Many authors differ between so-called simple elements with only nodal degrees of freedom and complex elements with degrees of freedom on the whole element. A unified formulation with an arbitrary number of degrees of freedom can be found in [18]. Davis *et al.* [5] presents a conventional 2-node isoparametric Timoshenko beam element.

It is clear, that in the spirit of a good compromise between computational cost and accuracy, the proper choice of ansatz-functions is an important task. A widely-observed phenomenon when simulating Timoshenko beams is the so-called shear locking. Displacement-based finite element formulations, especially if low-order ansatz-functions or polynomials of the same degree for displacement and rotation are used, tend to underestimate the displacements. This is because such elements can not model accurately the strain and therefore the strain energy. A survey on shear-locking can be found, for example, in [21]. There are several possible solutions for the shear-locking problem. First an under-integration can be performed to get closer to reality, see *e.g.* [23]. An improvement is the so-called selective reduced integration, where only certain terms are under-integrated, see [38], in which a four node Timoshenko beam element with selective reduced integration is presented. A different approach is shown in [31], where shear-locking is prevented posing the two polynomials modeling displacement and rotation interdependent. This seams reasonable, because those degrees of freedom are connected in the Timoshenko beam equations as well. Another approach is to use other or more degrees of freedom. Taylor *et al.* [30] uses a mixed finite element method (primal unknowns are now displacement, strain and stress). This way, strain and stress can have separate ansatz-functions with proper polynomial degree. A similar idea is used in [27], where a modified beam theory with other alternative unknowns to displacement and rotation is applied. Friedman and Kosmatka [9] provides a survey on techniques for solving the Timoshenko beam equations via discretization and how to avoid too stiff elements, *e.g.* by applying different order polynomials or reduced integration. Moreover two-node elements without shear locking for particular distributed loads are shown.

A more recent approach to determine ansatz-functions for the Timoshenko beam problem is to derive them directly from the beam problem leading to the so-called analytic ansatz-functions. An element based on analytic ansatz-functions is presented in [24], where a beam element is constructed from the homogeneous solution of the Timoshenko beam equations resulting in exact values of displacement and angle at nodes. This idea is also used in [20], where based on analytic ansatz-functions stiffness matrices are calculated and numerical tests with a cantilever are performed. Jelenić and Papa [14] and Papa Dukić and Jelenić [22] present analytic ansatz-functions as well. In [22], the Timoshenko beam equations are stated and analytically solved. The remaining constants are determined via boundary conditions and the stiffness matrix is calculated explicitly.

In our work, a finite element discretization with analytic ansatz-functions (comparable to [20] and [22]) is used. This approach results in locking-free 2-node Timoshenko beam elements. Consequently, no refinement of the element is required to prevent shear locking. Thus we can accurately model (thick) beams while still retaining computation times of the same order of magnitude as those for truss simulation for the solution of the whole network. In addition, we show that using these ansatz-functions we can solve not only the displacements and rotations of one beam element analytically, but those of the whole network. This is done in two steps, where in the first step the analytic solution for the network problem is constructed and in the second step it is shown that the nodal values of the analytic network solutions can be computed through the solution of a specific FE-type problem. From the obtained nodal values the full solution can be reconstructed simply by evaluating the chosen ansatz-functions on the individual beams.

Based on the beam network, we describe a topology optimization problem using the ground structure approach [6] and the SIMP-model [3] as well as multi-material optimization for beam networks, along the lines of [19,28,29]. The latter approach is also used in [12,13] for laminated composite materials.

The article concludes with numerical studies on the performance of the FE-type approach as well as test cases for the different structural optimization problems mentioned above.

2. Timoshenko beam model

Throughout the paper, the structural elements are modeled as linear Timoshenko beams with linear elastic constitutive behavior. The governing equation for the static equilibrium of a single, initially straight beam aligned along the E_1-axis with, *c.f.* Figure 1, length L is:

$$\left.\begin{aligned} \bar{N}(x_1) + N'(x_1) &= 0 \\ \bar{M}(x_1) + M'(x_1) + E_1 \times N(x_1) &= 0 \end{aligned}\right\} \quad x_1 \text{ in } (0, L). \tag{2.1}$$

The symbol $(\cdot)'$ denotes differentiation w.r.t. the spatial variable x_1, varying along the beam axis. $\bar{N}$ and $\bar{M}$ are distributed external loads and moments respectively. Constitutive equations are given as:

$$\begin{aligned} N(x_1) &= C_N(u'(x_1) + E_1 \times \phi(x_1)), \quad & C_N &:= \operatorname{diag}(EA, kGA, kGA), \\ M(x_1) &= C_M \phi'(x_1), & C_M &:= \operatorname{diag}(GI_t, EI_2, EI_3), \end{aligned} \tag{2.2}$$

connecting the kinematics to the primal unknowns $u : [0, L] \to \mathbb{R}^3$ and $\phi : [0, L] \to \mathbb{R}^3$, describing displacement of the centerline and the rotation of the cross section of the beam, respectively. By virtue of (2.2), N computes stress resultants for normal and shear forces and M does the same for torsion and bending moments. Material constants – assumed to be constant along the beam axis – are collected in the matrices C_N and C_M and are given as elastic and shear modulus E and G and the following geometric properties of the cross section: area of cross section A, corrected shear area kA with shear correction factor k as well as second and polar moments of area I_2, I_3 and I_t. For more details on equations (2.1) and (2.2), see, *e.g.* [20].

2.1. Modeling of a beam network

In order to build more complex structures out of beams, we must connect them physically with joints. Graphs are the mathematical tool used to describe such networks. Considering a set of n vertices $v_1, \ldots, v_n \in \mathbb{R}^3$ (the

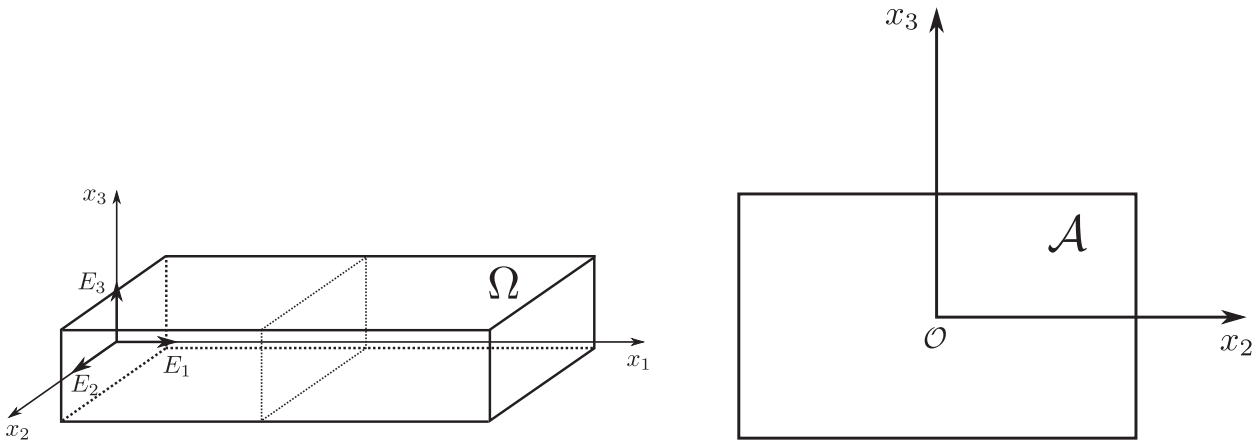

FIGURE 1. Beam in reference configuration with corresponding local coordinate system $\{E_1, E_2, E_3\}$ and its cross section $\mathcal{A}$.

joints) that are connected by m edges $b_1, \dots, b_m$ (the beams), we must formulate appropriate transmission conditions depending on the type of joint, see also [17].
The edges of the directed graph (since we parameterize the beams in a certain direction) are defined as a tuple of indices:

$$\forall i \in \mathcal{M} := \{1, \dots, m\}: \quad b_i = (i_1, i_2), \quad i_1, i_2 \in \mathcal{N} := \{1, \dots, n\}. \tag{2.3}$$

Here, the ith beam connects point v_{i_1} with v_{i_2} and the beam length is $L_i = \|v_{i_2} - v_{i_1}\|$. The actual initial position of a beam in space is described by a rigid body transformation (pure translations and rotation) of the reference domain $\Omega_i = [0, L_i] \times \mathcal{A}_i$. This transformation can be expressed by a function $x_c : [0, L_i] \to \mathbb{R}^3, x_1 \mapsto \frac{1}{L_i}(x_1 v_{i_2} + (L_i - x_1)v_{i_1})$, which maps midline to midline, and a function $x_A : \mathcal{A}_i \to \mathbb{R}^3, (x_2, x_3) \mapsto x_2 E_{i2} + x_3 E_{i3} v_{i_1}$, which maps cross section to cross section. Hence,

$$x = x_c(x_1) + x_A(x_2, x_3) \tag{2.4}$$

$$x(0) = v_{i_1}, \quad x(L_i) = v_{i_2}, \quad T_i := \nabla x = \begin{pmatrix} E_{i1} & E_{i2} & E_{i3} \end{pmatrix} \in SO(3). \tag{2.5}$$

Thus, in a local coordinate system with basis $\{E_{i1} := \frac{1}{L_i}(v_{i_2} - v_{i_1}), E_{i2}, E_{i3}\}$ and origin v_{i_1} the point x has coordinates (x_1, x_2, x_3). In these coordinate systems the beam equations hold for every $i \in \mathcal{M}$

$$\left.\begin{aligned} \bar{N}_i + N_i' = 0, \quad & N_i = C_{N_i}(u_i' + E_{i1} \times \phi_i) \\ \bar{M}_i + M_i' + E_{i1} \times N_i = 0, \quad & M_i = C_{M_i} \phi_i' \end{aligned}\right\}, \quad x_1 \in (0, L_i). \tag{2.6}$$

All quantities in (2.6) are given in the local basis $\{E_{i1}, E_{i2}, E_{i3}\}$. Thus the local state (u_i, ϕ_i) must be transformed via T_i to the global basis $\{e_1, e_2, e_3\}$ to formulate transmission conditions at the connecting points. Let

$$\mathcal{M}^j := \{i \in \mathcal{M} : b_{i1} = j\} \cup \{i \in \mathcal{M} : b_{i2} = j\} =: \mathcal{M}_0^j \cup \mathcal{M}_L^j, \quad \forall j \in \mathcal{N},$$

be the index set of beams that are connected to node v_j ($\mathcal{M}_0^j$ the starting and $\mathcal{M}_L^j$ the ending beams, $\mathcal{M}_0^j \cap \mathcal{M}_L^j = \varnothing$) and

$$x_i^j := \begin{cases} 0, & i \in \mathcal{M}_0^j \\ L_i, & i \in \mathcal{M}_L^j \end{cases}, \qquad n_i^j := \begin{cases} -1, & i \in \mathcal{M}_0^j \\ 1, & i \in \mathcal{M}_L^j \end{cases}$$

be corresponding switching variables for $j \in \mathcal{N}$. We can now formulate continuity of displacements at joints (which is clearly a requirement if the beams are to stay connected at their endpoints, *i.e.* no sliding):

$$\forall k \in \mathcal{N}: \quad T_i u_i(x_i^k) = T_j u_j(x_j^k), \quad i,j \in \mathcal{M}^k. \tag{2.7}$$

Here, we restrict the problem to rigid joints, which implies continuity of rotations:

$$\forall k \in \mathcal{N}: \quad T_i \phi_i(x_i^k) = T_j \phi_j(x_j^k), \quad i,j \in \mathcal{M}^k. \tag{2.8}$$

If we define the vector of the state in local and global coordinates as follows

$$y_i(x_1) := \tilde{T}_i Y_i(x_1) := \tilde{T}_i \begin{pmatrix} u_i(x_1) \\ \phi_i(x_1) \end{pmatrix}, \quad \text{with } \tilde{T}_i := \begin{pmatrix} T_i & 0 \\ 0 & T_i \end{pmatrix}, \tag{2.9}$$

we can write equations (2.7) and (2.8) in compact form:

$$\forall k \in \mathcal{N}: \quad y_i(x_i^k) = y_j(x_j^k), \quad i,j \in \mathcal{M}^k, \tag{2.10}$$

and identify the global state of the beam network at node v_k with this common value $\bar{y}_k$. In this case joints also transport forces and moments, so that at equilibrium all incoming forces and moments have to be balanced at every free node. These conditions at free nodes can also be interpreted as a homogeneous Neumann condition; accordingly these nodes are also considered as Neumann nodes. We denote the corresponding index set by $\mathcal{N}_N \subset \mathcal{N}$. All other nodes are of Dirichlet type ($\mathcal{N}_D = \mathcal{N} \setminus \mathcal{N}_N$).

$$\forall j \in \mathcal{N}_N: \qquad \sum_{i \in \mathcal{M}^j} n_i^j f_i(x_i^j) = f_{N_j}, \qquad f_i := \tilde{T}_i \begin{pmatrix} N_i \\ M_i \end{pmatrix}, \tag{2.11}$$

$$\forall j \in \mathcal{N}_D: \qquad y_i(x_i^j) = y_{D_j}, \qquad i \in \mathcal{M}^j \tag{2.12}$$

where f_{N_j} is a given external load (force and moment defined in the global basis) acting at node v_j and y_{D_j} is a prescribed global state.

It should be noted that for every single component of the state variables u and ϕ different boundary conditions may apply, so that *e.g.* a node could be fixed in space (Dirichlet for displacement) but could rotate freely (Neumann for rotation). Solely for the sake of simplicity we restrict the problem to pure Neumann or Dirichlet conditions, note however that all theoretical statements in the following section carries over without further modification to this slightly more general situation.

2.2. Efficient numerical solution

This part of the paper presents a finite element approach that yields the analytic solution $\bar{y}_k$ at the nodes of the network without discretizing the single beams.

The main requirements of an optimization of large beam networks are clearly fast and accurate solutions. Usually the edges are discretized with finite elements (FE), constructed with standard interpolating shape functions, *e.g.* linear. Using the transmission conditions, a huge linear system of equations is constructed and solved. The main drawback of this method is, that with these shape functions an underestimation of displacements occurs, termed shear-locking, see *e.g.* [21]. This means that a highly refined FE-grid is required on every beam in order to obtain accurate solutions. This contradicts the previously mentioned requirements.

The approach chosen here thus follows three steps to demonstrate that with certain special shape functions the FE procedure yields analytic solutions to the beam network problem at every node of the graph:

(1) First we show that the state of the whole network is entirely determined by the global state $\bar{y}_k, k \in \mathcal{N}$, at the nodes.

(2) We conclude that the analytic solution to the beam network problem at the nodes can be computed by solving a linear system of equations of dimension $6|\mathcal{N}_N|$.
(3) We demonstrate that this approach is equivalent to a finite element method, where only one finite element with a special shape function per beam is used. We call these functions analytic shape functions.

Statement 1 requires us to demonstrate existence and uniqueness of solutions on a single edge and we therefore concentrate on the generic beam problem (subscript dropped), $x_1 \in (0, L)$,

$$\begin{aligned} \bar{N}(x_1) + N'(Y(x_1)) &= 0 \\ \bar{M}(x_1) + M'(Y(x_1)) + E_1 \times N(Y(x_1)) &= 0 \end{aligned} \tag{2.13}$$

with linear constitutive laws

$$\begin{aligned} N(Y(x_1)) &= C_N(u'(x_1) + E_1 \times \phi(x_1)) \\ M(Y(x_1)) &= C_M \phi'(x_1) \end{aligned} \tag{2.14}$$

and Dirichlet conditions for the state $Y(x_1)$ on both sides

$$Y(0) = Y_0, \quad Y(L) = Y_L. \tag{2.15}$$

We now split the solution $Y(x_1)$ into parts: $Y^h(x_1) = (u^h(x_1)^T, \phi^h(x_1)^T)^T$ corresponding to the Dirichlet conditions and the beam problem without distributed loads and $Y^p(x_1) = (u^p(x_1)^T, \phi^p(x_1)^T)^T$, with homogeneous Dirichlet conditions fulfilling the beam equations with distributed loads $\bar{F}(x_1) := (\bar{N}(x_1)^T, \bar{M}(x_1)^T)^T$. Due to the linearity of $N(Y)$ and $M(Y)$ w.r.t. Y it is clear that, if $Y^h(x_1)$, with $Y^h(0) = Y_0$ and $Y^h(L) = Y_L$, solves

$$\begin{aligned} N'(Y^h(x_1)) &= 0 \\ M'(Y^h(x_1)) + E_1 \times N(Y^h(x_1)) &= 0 \end{aligned} \tag{2.16}$$

and $Y^p(x_1)$, with $Y^p(0) = Y^p(L) = 0$, solves

$$\begin{aligned} \bar{N}(x_1) + N'(Y^p(x_1)) &= 0 \\ \bar{M}(x_1) + M'(Y^p(x_1)) + E_1 \times N(Y^p(x_1)) &= 0, \end{aligned} \tag{2.17}$$

the sum $Y(x_1) = Y^h(x_1) + Y^p(x_1)$ solves the beam problem (2.13)–(2.15).

For any boundary data Y_0, Y_L there is a unique smooth solution $Y^h(x_1) \in \mathcal{C}^2(0, L)$, since problem (2.16), (2.14) may be rewritten as a first order system of linear ordinary differential equations (ODEs). This is done by integrating equations (2.16)

$$\begin{aligned} N'(Y^h) = 0 \quad &\Rightarrow \quad N(Y^h) = c_1 \\ M'(Y^h) = c_1 \times E_1 \quad &\Rightarrow \quad M(Y^h) = x_1(c_1 \times E_1) + c_2 \end{aligned} \tag{2.18}$$

(c_1 and c_2 as yet unspecified integration constants) and together with the linear constitutive laws we obtain

$$\begin{aligned} C_N((u^h)' + E_1 \times \phi^h) &= c_1 \\ C_M(\phi^h)' &= c_2 + x_1(c_1 \times E_1), \end{aligned}$$

which is equivalent to

$$\begin{pmatrix} u^h \\ \phi^h \end{pmatrix}' = \begin{pmatrix} 0 & -\hat{E}_1 \\ 0 & 0 \end{pmatrix} \begin{pmatrix} u^h \\ \phi^h \end{pmatrix} + \begin{pmatrix} C_N^{-1} & 0 \\ 0 & C_M^{-1} \end{pmatrix} \begin{pmatrix} c_1 \\ c_2 + x_1(c_1 \times E_1) \end{pmatrix}.$$

Here $\hat{E}_1 v = E_1 \times v$, $\forall v \in \mathbb{R}^3$, represents the cross product as matrix multiplication. This may now be recast as a system of linear ODEs:

$$(Y^h)'(x_1) = AY^h(x_1) + B(x_1)c, \qquad x_1 \in (0, L), \tag{2.19}$$

where

$$A := \begin{pmatrix} 0 & -\hat{E}_1 \\ 0 & 0 \end{pmatrix}, \qquad B := \begin{pmatrix} C_N^{-1} & 0 \\ 0 & C_M^{-1} \end{pmatrix} \begin{pmatrix} I & 0 \\ -x_1\hat{E}_1 & I \end{pmatrix}, \qquad c := \begin{pmatrix} c_1 \\ c_2 \end{pmatrix}.$$

Its solution is explicitly given by

$$Y^h(x_1) = \exp(Ax_1)\Bigg(Y_0 + \underbrace{\int_0^{x_1} \exp(-A\xi)B(\xi)\mathrm{d}\xi}_{:=D(x_1)}\, c\Bigg). \tag{2.20}$$

We note that A is nilpotent ($A^2 = 0$), so that

$$\exp(Ax_1) = I + x_1 A = \begin{pmatrix} I & -x_1\hat{E}_1 \\ 0 & I \end{pmatrix} \quad \Rightarrow \quad B = \begin{pmatrix} C_N^{-1} & 0 \\ 0 & C_M^{-1} \end{pmatrix} \exp(-Ax_1)^T, \tag{2.21}$$

which implies the symmetry and invertibility of $D(x_1)$ (and its inverse) for $0 \le x_1 \le L$. To fulfill both boundary conditions we choose c such that $Y^h(L) = Y_L$:

$$Y_L = \exp(AL)[Y_0 + D(L)c] \quad \Leftrightarrow \quad c = D^{-1}(L)(\exp(-AL)Y_L - Y_0). \tag{2.22}$$

As a consequence we construct $Y^h(x_1)$ depending on the boundary conditions so that

$$\begin{aligned} Y^h(x_1) &= \exp(Ax_1)\Big(Y_0 + D(x_1)D^{-1}(L)\big(\exp(-AL)Y_L - Y_0\big)\Big) \\ &= \exp(Ax_1)\left(I - D(x_1)D^{-1}(L),\, D(x_1)D^{-1}(L)\exp(-AL)\right)\begin{pmatrix} Y_0 \\ Y_L \end{pmatrix} \\ &=: H(x_1)\begin{pmatrix} Y_0 \\ Y_L \end{pmatrix}, \quad H(x_1) := \begin{pmatrix} H_u(x_1) \\ H_\phi(x_1) \end{pmatrix}, \end{aligned} \tag{2.23}$$

which can be interpreted as a shape function for a two-node finite element. Indeed, we call $H(x_1)$ an analytic shape function, since it analytically solves the beam equations without distributed loads.

The same procedure may be applied to transform problem (2.17) together with (2.14) into a first order system of linear ODEs, which then reads as

$$(Y^p)'(x_1) = AY^p(x_1) + \bar{b}(x_1) + B(x_1)\bar{c}, \qquad x_1 \in (0, L), \tag{2.24}$$

where the new introduced vector $\bar{b}(x_1)$ emerges from integrating the distributed loads:

$$\bar{b}(x_1) := \begin{pmatrix} C_N^{-1} & 0 \\ 0 & C_M^{-1} \end{pmatrix} \begin{pmatrix} -\int_0^{x_1} \bar{N}(\xi)\mathrm{d}\xi \\ -\int_0^{x_1} \bar{M}(\xi)\mathrm{d}\xi + \hat{E}_1 \int_0^{x_1}\int_0^{\xi} \bar{N}(\zeta)\mathrm{d}\zeta\mathrm{d}\xi \end{pmatrix}. \tag{2.25}$$

We need to ensure that $\bar{b} \in \mathcal{C}^1(0, L)$, so that the solution $Y^p \in \mathcal{C}^2(0, L)$ is a classical solution to the beam problem. Therefore, the distributed loads have to be at least continuous over a beam. Then the arguments applied previously ensure existence and uniqueness of the solution $Y^p(x_1)$ and also for the sum $Y(x_1) = Y^h(x_1) + Y^p(x_1)$. To conclude statement 1 we note that from the global states $\bar{y}_k$ at the nodes the local states at the ends of each beam can be calculated and therefore the whole beam net is uniquely determined.

Statement 2 requires an additional fulfillment of the continuity conditions for local states at nodes (2.10) and balance of forces and moments at free nodes (2.11). Continuity can be trivially fulfilled by introducing the common state $\bar{y}_k$ at nodes as unknowns of the problem, knowing that the underlying beam equations can be

solved uniquely for any given configuration. Let

$$\bar{y} := \begin{pmatrix} \bar{y}_1 \\ \vdots \\ \bar{y}_n \end{pmatrix}, \qquad \bar{y}_i = y_{D_i}, \quad i \in \mathcal{N}_D,$$
$$\bar{f} := \begin{pmatrix} f_{N_1} \\ \vdots \\ f_{N_n} \end{pmatrix}, \quad f_{N_i} = 0, \quad i \in \mathcal{N}_D$$

be the vector of nodal states and the vector of nodal loads (in part given explicitly as Neumann conditions). With this definition the Dirichlet boundary conditions are also incorporated into the solution $\bar{y}$, which has to be chosen such that the nodal balance of forces and moments is fulfilled. In order to rewrite these conditions in terms of $\bar{y}$, we need to construct a mapping of the state at both ends of each beam to the internal forces/moments at both ends that is in accordance to the beam equations:

$$\begin{pmatrix} \bar{y}_{i_1} \\ \bar{y}_{i_2} \end{pmatrix} = \tilde{\tilde{T}}_i \begin{pmatrix} Y_{i0} \\ Y_{iL} \end{pmatrix} \longmapsto \tilde{\tilde{T}}_i \begin{pmatrix} -F_i(0) \\ F_i(L_i) \end{pmatrix} = \begin{pmatrix} -f_i(0) \\ f_i(L_i) \end{pmatrix}, \ \tilde{\tilde{T}}_i := \begin{pmatrix} \tilde{T}_i & 0 \\ 0 & \tilde{T}_i \end{pmatrix}. \tag{2.26}$$

To this end, we split the local inner forces $F_i(Y_i(x_1))$ due to linearity as follows

$$F_i(x_1) := F_i(Y_i(x_1)) = F_i(Y_i^h(x_1) + Y_i^p(x_1)) = \underbrace{F_i(Y_i^h(x_1))}_{=:F_i^h(x_1)} + \underbrace{F_i(Y_i^p(x_1))}_{=:F_i^p(x_1)}, \tag{2.27}$$

where $F_i^p(x_1)$ does not depend on the solution and may be calculated in advance. From calculation (2.18) we know that we can write inner forces/moments as:

$$F_i^h(x_1) = \begin{pmatrix} N_i(Y_i^h(x_1)) \\ M_i(Y_i^h(x_1)) \end{pmatrix} = \begin{pmatrix} c_{i1} \\ c_{i2} + x_1(c_{i1} \times E_{i1}) \end{pmatrix} = \exp(-Ax_1)c_i \tag{2.28}$$

and therefore

$$\begin{pmatrix} -F_i^h(0) \\ F_i^h(L_i) \end{pmatrix} = \begin{pmatrix} -I \\ \exp(-AL_i)^T \end{pmatrix} c_i \tag{2.29}$$
$$= \begin{pmatrix} -I \\ \exp(-AL_i)^T \end{pmatrix} D_i^{-1}(L_i)(\exp(-AL_i)Y_{iL} - Y_{i0}) \tag{2.30}$$
$$= \begin{pmatrix} -I \\ \exp(-AL_i)^T \end{pmatrix} D_i^{-1}(L_i) \left(-I, \exp(-AL_i)\right) \begin{pmatrix} Y_{i0} \\ Y_{iL} \end{pmatrix} \tag{2.31}$$
$$=: K_i^{\mathrm{loc}} \begin{pmatrix} Y_{i0} \\ Y_{iL} \end{pmatrix}, \qquad K_i^{\mathrm{loc}} \in \mathbb{R}^{12\times 12} \text{ symmetric.} \tag{2.32}$$

We have therefore explicitly constructed mapping (2.26) as

$$\begin{pmatrix} -f_i(0) \\ f_i(L_i) \end{pmatrix} = \tilde{\tilde{T}}_i \, (K_i^{\mathrm{loc}}) \, \tilde{\tilde{T}}_i^T \begin{pmatrix} \bar{y}_{i_1} \\ \bar{y}_{i_2} \end{pmatrix} + \underbrace{\tilde{\tilde{T}}_i \begin{pmatrix} -F_i^p(0) \\ F_i^p(L_i) \end{pmatrix}}_{=:\tilde{f}_i}, \tag{2.33}$$

which is affine linear w.r.t. the states at the nodes. Now we are able to formulate the nodal balance conditions (2.11) as a linear system of equations that incorporates $6|\mathcal{N}_N|$ equations. To this end, let P_i be the boolean matrix that projects $\bar{y}$ onto the two nodal states of the ith beam:

$$\begin{pmatrix} \bar{y}_{i_1} \\ \bar{y}_{i_2} \end{pmatrix} = P_i \bar{y}, \qquad P_i \in \{0,1\}^{12\times 6n}. \tag{2.34}$$

Likewise $P_N \in \{0,1\}^{6|\mathcal{N}_N| \times 6n}$ is the matrix that extracts the states of all free/Neumann nodes y_N and $P_D \in \{0,1\}^{6|\mathcal{N}_D| \times 6n}$ is the analogue for Dirichlet points y_D, with

$$\bar{y} = P_N^T y_N + P_D^T y_D. \tag{2.35}$$

We can recast (2.11) equivalently as

$$P_N \underbrace{\left(\sum_{i=1}^{m} P_i^T \tilde{\tilde{T}}_i (K_i^{\text{loc}}) \tilde{\tilde{T}}_i^T P_i \right)}_{:=\tilde{K}} (P_N^T y_N + P_D^T y_D) + P_N \underbrace{\sum_{i=1}^{m} P_i^T \tilde{f}_i}_{=:\tilde{f}} = P_N \bar{f} \tag{2.36}$$

and can solve for the states at the free nodes that are not directly given by Dirichlet boundary conditions. We end up with the following linear system of equations:

$$\left(P_N \tilde{K} P_N^T \right) y_N = P_N(\bar{f} - \tilde{f}) - \left(P_N \tilde{K} P_D^T \right) y_D \quad \Leftrightarrow \quad Ky = f. \tag{2.37}$$

We note again that by solving (2.37), the analytic solution at all free nodes of the beam network problem is calculated, which concludes statement (2).

Statement 3 requires us to show that the linear system of equations produced by the FE method – by discretizing the weak form of the local beam equations with proper shape functions – yields the same as (2.37). Since the matrix assembly with local stiffness matrices describing a single beam defined through its states at the ends is already in perfect analogy to a standard FE procedure, we only have to verify that the discretized weak form yields an exact mapping from nodal states to inner forces/moments at the ends. If this holds true, then by construction we obtain the analytic solution at the nodes by solving the corresponding linear system of equations. Since

$$u(x_1) = u^h(x_1) + u^p(x_1) = H_u(x_1) \begin{pmatrix} Y_0 \\ Y_L \end{pmatrix} + u^p(x_1) \tag{2.38}$$

$$\phi(x_1) = \phi^h(x_1) + \phi^p(x_1) = H_\phi(x_1) \begin{pmatrix} Y_0 \\ Y_L \end{pmatrix} + \phi^p(x_1) \tag{2.39}$$

solve the beam equations, we have for every beam (although subscript i is omitted):

$$\begin{aligned}
& 0 = \bar{N} + N'(Y) \qquad \wedge \qquad 0 = \bar{M} + M'(Y) + E_1 \times N(Y) \\
\Rightarrow \quad & 0 = H_u^T(\bar{N} + N'(Y)) + H_\phi^T(\bar{M} + M'(Y) + E_1 \times N(Y)) \\
& = H_u^T \bar{N} + H_\phi^T \bar{M} + H_u^T N'(Y) + H_\phi^T(M'(Y) + \hat{E}_1 N(Y)) \\
& = \int_0^L H_u^T \bar{N} + H_\phi^T \bar{M} \mathrm{d}x_1 + \int_0^L H_u^T N'(Y) + H_\phi^T(M'(Y) - \hat{E}_1^T N(Y)) \mathrm{d}x_1 \\
& = \int_0^L H^T \bar{F} \mathrm{d}x_1 + \int_0^L H_u^T N'(Y) + H_\phi^T M'(Y) - (\hat{E}_1 H_\phi)^T N(Y) \mathrm{d}x_1 \\
& = \int_0^L H^T \bar{F} \mathrm{d}x_1 + [H_u^T N(Y)]_0^L + [H_\phi^T M(Y)]_0^L \\
& \quad - \int_0^L (H_u')^T N(Y) + (H_\phi')^T M(Y) + (\hat{E}_1 H_\phi)^T N(Y) \mathrm{d}x_1
\end{aligned}$$

$$= \int_0^L H^T \bar{F} \mathrm{d}x_1 + \begin{pmatrix} -N(Y(0)) \\ -M(Y(0)) \\ N(Y(L)) \\ M(Y(L)) \end{pmatrix} - \int_0^L (H'_u + \hat{E}_1 H_\phi)^T N(Y) + (H'_\phi)^T M(Y) \mathrm{d}x_1.$$

The last step is valid as $H_u(0) = (I, 0, 0, 0)$, $H_u(L) = (0, 0, I, 0), \ldots$ must reproduce the boundary conditions (2.12). We proceed to analyze the last integral of the equation above:

$$\begin{aligned}
&\int_0^L (H'_u + \hat{E}_1 H_\phi)^T N(Y) + (H'_\phi)^T M(Y) \mathrm{d}x_1 \\
&\quad = \int_0^L (H'_u + \hat{E}_1 H_\phi)^T N(Y^h + Y^p) + (H'_\phi)^T M(Y^h + Y^p) \mathrm{d}x_1 \\
&\quad = \int_0^L (H'_u + \hat{E}_1 H_\phi)^T N(Y^h) + (H'_\phi)^T M(Y^h) \mathrm{d}x_1 + \\
&\qquad + \int_0^L (H'_u + \hat{E}_1 H_\phi)^T N(Y^p) + (H'_\phi)^T M(Y^p) \mathrm{d}x_1 \\
&\quad = \int_0^L (H'_u + \hat{E}_1 H_\phi)^T C_N (H'_u + \hat{E}_1 H_\phi) + (H'_\phi)^T C_M H'_\phi \mathrm{d}x_1 \begin{pmatrix} Y_0 \\ Y_L \end{pmatrix} + \\
&\qquad + \int_0^L (H'_u + \hat{E}_1 H_\phi)^T C_N ((u^p)' + \hat{E}_1 \phi^p) + (H'_\phi)^T C_M (\phi^p)' \mathrm{d}x_1.
\end{aligned}$$

After rearranging the terms of the last summand of the above equation and integrating by parts, we obtain:

$$\begin{aligned}
&\int_0^L (H'_u + \hat{E}_1 H_\phi)^T C_N ((u^p)' + \hat{E}_1 \phi^p) + (H'_\phi)^T C_M (\phi^p)' \mathrm{d}x_1 \\
&\quad = \underbrace{[(H'_u + \hat{E}_1 H_\phi)^T C_N u^p]_0^L + [(H'_\phi)^T C_M \phi^p]_0^L}_{=0, \text{ boundary conditions of } Y^p(x_1)} - \\
&\qquad - \int_0^L [C_N (H''_u + \hat{E}_1 H'_\phi)]^T u^p + [C_M (H''_\phi) + \hat{E}_1 C_N (H'_u + \hat{E}_1 H_\phi)]^T \phi^p \mathrm{d}x_1 = 0.
\end{aligned}$$

The last integral vanishes because of the construction of the analytic shape functions:

$$\begin{aligned}
C_N (H''_u + \hat{E}_1 H'_\phi) \begin{pmatrix} Y_0 \\ Y_L \end{pmatrix} &= N'(Y^h) = 0 \\
[C_M (H''_\phi) + \hat{E}_1 C_N (H'_u + \hat{E}_1 H_\phi)] \begin{pmatrix} Y_0 \\ Y_L \end{pmatrix} &= M'(Y^h) + \hat{E}_1 N(Y^h) = 0 \\
&\forall Y_0, Y_L \in \mathbb{R}^6.
\end{aligned} \tag{2.40}$$

Combining everything, we again have an exact mapping of states at the end of each beam to the resulting forces/moments as in (2.26), which is required to formulate the exact balance of force/momentum at nodes, (2.11). Additionally, it is exactly the weak form of the beam problem discretized by the analytic shape functions $H(x_1)$ and thus equivalent to the FE method.

$$\begin{pmatrix} -F(Y(0)) \\ F(Y(L)) \end{pmatrix} = \int_0^L (H_u' + \hat{E}_1 H_\phi)^T C_N (H_u' + \hat{E}_1 H_\phi) + (H_\phi')^T C_M (H_\phi') \mathrm{d}x_1 \begin{pmatrix} Y_0 \\ Y_L \end{pmatrix} - \int_0^L H^T \bar{F} \mathrm{d}x_1. \tag{2.41}$$

As this has to hold true for all states Y_0, Y_L at the ends, we can conclude that

$$K^{\mathrm{loc}} = \int_0^L (H_u' + \hat{E}_1 H_\phi)^T C_N (H_u' + \hat{E}_1 H_\phi) + (H_\phi')^T C_M (H_\phi') \mathrm{d}x_1 \tag{2.42}$$

$$\begin{pmatrix} -F_i^p(0) \\ F_i^p(L_i) \end{pmatrix} = - \int_0^L H^T \bar{F} \mathrm{d}x_1, \tag{2.43}$$

and that exactly the same linear system of equations is obtained as from the direct construction (2.37). In contrast to the direct approach above, in this setting it is not necessary to construct the part of the solution accounting for distributed loads $Y^p(x_1)$. This concludes statement 3.

The analytic shape functions H_u and H_ϕ given in (2.23) allow an exact integration in the assembly of the local stiffness matrix K^{loc} (2.42). In (2.43), a sufficiently accurate numerical quadrature rule must be chosen depending on the given distributed load $\bar{F}$. If the distributed load can be exactly integrated, for example, loads given by a polynomial function of x_1, then we obtain a fully analytic solution scheme. Consequently, no spatial discretization of an individual beam is necessary. On the other hand, the analytic solution approach on the network is clearly limited by the necessity to prescribe a linear constitutive law as well as the small displacement assumption. As consequence, problems with a serious constitutive or geometric nonlinearity, see [25], cannot be treated by our approach in a straightforward way.

3. Optimization

In this section we present optimization models for topology and multi-material optimization of beam networks. The underlying simulation model is a network of Timoshenko beams as described in Section 2.

3.1. Topology optimization using the SIMP-approach

First we describe the minimum-compliance (or maximum stiffness) topology optimization problem for a 3D ground structure. Is is assumed, but not necessary, that all elements are made of the same material. As in Section 2.1, we consider a beam network geometry with a set of n nodal points and m possible connections between points, as well as loads and boundary conditions (ground structure approach). From now on, we assume that our structure is loaded with a constant distributed external load, *e.g.* gravity, and no distributed moments. Thus we have on every bar:

$$\begin{aligned} \bar{N}_i(x_1) &= \begin{pmatrix} \bar{N}_{i1} \\ \bar{N}_{i2} \\ \bar{N}_{i3} \end{pmatrix} \ \forall i, \\ \bar{M}_i(x_1) &= 0 \ \forall i. \end{aligned} \tag{3.1}$$

In addition, nodal forces $\bar{f}$ can be given, see statement 2 of Section 2.2. Now let K_i^{loc} be the local stiffness matrix of bar i. It can be calculated either using the direct derivation from the Timoshenko ordinary differential equations, which can be found in (2.30)–(2.32) employing (2.20) and (2.21), or using the straight-forward alternative with the finite element method, which can be found in (2.42). In addition, (2.23) shows the derivation of the analytic shape functions. Whichever method is employed, the resulting matrix reads (with subscript

i omitted)

$$K^{\text{loc}} = \begin{pmatrix} k_1 & 0 & 0 & 0 & 0 & 0 & -k_1 & 0 & 0 & 0 & 0 & 0 \\ 0 & d_1 & 0 & 0 & 0 & d_2 & 0 & -d_1 & 0 & 0 & 0 & d_2 \\ 0 & 0 & d_1 & 0 & -d_2 & 0 & 0 & 0 & -d_1 & 0 & -d_2 & 0 \\ 0 & 0 & 0 & k_2 & 0 & 0 & 0 & 0 & 0 & -k_2 & 0 & 0 \\ 0 & 0 & -d_2 & 0 & d_3 & 0 & 0 & 0 & d_2 & 0 & d_4 & 0 \\ 0 & d_2 & 0 & 0 & 0 & d_3 & 0 & -d_2 & 0 & 0 & 0 & d_4 \\ -k_1 & 0 & 0 & 0 & 0 & 0 & k_1 & 0 & 0 & 0 & 0 & 0 \\ 0 & -d_1 & 0 & 0 & 0 & -d_2 & 0 & d_1 & 0 & 0 & 0 & -d_2 \\ 0 & 0 & -d_1 & 0 & d_2 & 0 & 0 & 0 & d_1 & 0 & d_2 & 0 \\ 0 & 0 & 0 & -k_2 & 0 & 0 & 0 & 0 & 0 & k_2 & 0 & 0 \\ 0 & 0 & -d_2 & 0 & d_4 & 0 & 0 & 0 & d_2 & 0 & d_3 & 0 \\ 0 & d_2 & 0 & 0 & 0 & d_4 & 0 & -d_2 & 0 & 0 & 0 & d_3 \end{pmatrix}, \tag{3.2}$$

where

$$\begin{aligned} k_1 &:= \frac{EA}{L} & k_2 &:= \frac{GI_t}{L} \\ d_1 &:= d_5\, 12kGA & d_2 &:= d_5\, 6LkGA \\ d_3 &:= d_5\, (12EI + 4L^2kGA) & d_4 &:= d_5\, (2L^2kGA - 12EI) \\ d_5 &:= \frac{EI}{L\,(12EI + L^2kGA)}. \end{aligned} \tag{3.3}$$

It is also possible to obtain a block structure in matrix K^{loc} if the entries of the vector of unknowns are rearranged. From now on we assume that homogeneous Dirichlet boundary conditions of the type $y_{D_i} = 0\ \forall i \in \mathcal{N}_D$ hold. Then the state problem (2.36) reads:

$$\begin{aligned} & P_N \left(\sum_{i=1}^{m} P_i^T \tilde{\tilde{T}}_i (K_i^{\text{loc}}) \tilde{\tilde{T}}_i^T P_i \right) P_N^T y_N + P_N \sum_{i=1}^{m} P_i^T \tilde{f}_i = P_N \bar{f} \\ \Leftrightarrow \quad & \left(\sum_{i=1}^{m} P_N P_i^T \tilde{\tilde{T}}_i (K_i^{\text{loc}}) \tilde{\tilde{T}}_i^T P_i P_N^T \right) y_N = P_N \bar{f} - \sum_{i=1}^{m} P_N P_i^T \tilde{f}_i. \end{aligned} \tag{3.4}$$

We further define $\hat{K}_i^{\text{loc}} := P_N P_i^T \tilde{\tilde{T}}_i (K_i^{\text{loc}}) \tilde{\tilde{T}}_i^T P_i P_N^T$, $\hat{f}_i^{\text{dist}} := -P_N P_i^T \tilde{f}_i$ and $\hat{f}^{\text{nod}} := P_N \bar{f}$, resulting in the following linear system of equations (with the subscript N dropped from y):

$$\left(\sum_{i=1}^{m} \hat{K}_i^{\text{loc}} \right) y = \hat{f}^{\text{nod}} + \sum_{i=1}^{m} \hat{f}_i^{\text{dist}} \tag{3.5}$$

or

$$Ky = f, \tag{3.6}$$

where we have used $K := \sum_{i=1}^{m} \hat{K}_i^{\text{loc}}$ and $f := \hat{f}^{\text{nod}} + \sum_{i=1}^{m} \hat{f}_i^{\text{dist}}$. For optimization, we introduce a set of design variables $\alpha_i,\ i = 1, 2, \dots m$, with which we linearly scale the material properties of each bar. Along with these variables, we have box-constraints of the type

$$0 < \alpha_{\min} \leq \alpha_i \leq 1\ \forall i, \tag{3.7}$$

where $\alpha_{\min}$ is a small positive constant. In order to obtain an approximate 0-1-solution with a certain (low) number of beams in the sense that the material properties are either on the lower bound (*i.e.* the bar disappears), or on the upper bound (*i.e.* the bar is made from the unscaled material properties, given in (3.3)), the well-known SIMP model [3] is utilized. To do this, the design variables are penalized. The final parametrized state

problem including the penalization parameter $p \in \mathbb{N}$ reads as follows:

$$\left(\sum_{i=1}^{m} \alpha_i^p \hat{K}_i^{\mathrm{loc}}\right) y(\alpha) = \hat{f}^{\mathrm{nod}} + \sum_{i=1}^{m} \alpha_i^p \hat{f}_i^{\mathrm{dist}}. \tag{3.8}$$

Note that the sum of the distributed forces $\hat{f}_i^{\mathrm{dist}}$ depends on the design, but the fixed nodal forces $\hat{f}^{\mathrm{nod}}$ are design-independent. Finally, a resource constraint of the type

$$\sum_{i}^{m} \alpha_i V_i \leq V, \tag{3.9}$$

with V_i, $i = 1 \dots m$ being the beam volumes, is added. As objective, we introduce the well-known compliance functional, which describes the overall stiffness of the structure subjected to the given loads. Hence, we consider the displacement of the structure in the direction of the given nodal forces $\hat{f}^{\mathrm{nod}}$, which is described by the scalar product:

$$c_1(\alpha, y(\alpha)) := (\hat{f}^{\mathrm{nod}})^T y(\alpha). \tag{3.10}$$

In addition, we have to take into account the displacement of every beam i in direction of the distributed force $\bar{N}_i$. We denote by $u_i(x_1, \alpha)$ the local displacement of beam i, which, by application of (2.38), can be decomposed into a design-dependent part $u_i^h(x_1, \alpha)$ and a design-independent part $u_i^p(x_1)$, where the latter is design-independent because the local distributed force and the material properties are scaled by the same factor α_i^p. Then we obtain:

$$\begin{aligned}
&\sum_{i=1}^{m} \int_0^L \alpha_i^p (\bar{N}_i)^T u_i(x_1, \alpha)\, \mathrm{d}x_1 \\
\overset{(2.38)}{=}\ &\sum_{i=1}^{m} \int_0^L \alpha_i^p (\bar{N}_i)^T (u_i^h(x_1, \alpha) + u_i^p(x_1))\, \mathrm{d}x_1 \\
\overset{(2.38)}{=}\ &\sum_{i=1}^{m} \left(\int_0^L \alpha_i^p (\bar{N}_i)^T H_{u,i}(x_1) \begin{pmatrix} Y_{i0}(\alpha) \\ Y_{iL}(\alpha) \end{pmatrix} \mathrm{d}x_1 + \int_0^L \alpha_i^p (\bar{N}_i)^T u_i^p(x_1)\, \mathrm{d}x_1 \right).
\end{aligned} \tag{3.11}$$

The first integral in (3.11) can be rewritten as

$$\begin{aligned}
&\sum_{i=1}^{m} \int_0^L \alpha_i^p (\bar{N}_i)^T H_{u,i}(x_1)\, \mathrm{d}x_1 \begin{pmatrix} Y_{i0}(\alpha) \\ Y_{iL}(\alpha) \end{pmatrix} \\
\overset{(2.43)}{=}\ &\sum_{i=1}^{m} -\alpha_i^p \begin{pmatrix} -F_i^p(0) \\ F_i^p(L_i) \end{pmatrix}^T \begin{pmatrix} Y_{i0}(\alpha) \\ Y_{iL}(\alpha) \end{pmatrix}.
\end{aligned} \tag{3.12}$$

Using (2.26), (2.34), (2.35) and the definition of $\hat{f}_i^{\mathrm{dist}}$ above, the right hand side of (3.12) can be rewritten in global quantities as follows:

$$\begin{aligned}
&\sum_{i=1}^{m} -\alpha_i^p \begin{pmatrix} -F_i^p(0) \\ F_i^p(L_i) \end{pmatrix}^T \begin{pmatrix} Y_{i0}(\alpha) \\ Y_{iL}(\alpha) \end{pmatrix} \\
=\ &\sum_{i=1}^{m} -\alpha_i^p \begin{pmatrix} -F_i^p(0) \\ F_i^p(L_i) \end{pmatrix}^T \widetilde{\widetilde{T}}_i^T P_i P_N^T\, y(\alpha) \\
=\ &\sum_{i=1}^{m} \alpha_i^p (\hat{f}_i^{\mathrm{dist}})^T y(\alpha) =: c_2(\alpha, y(\alpha)).
\end{aligned} \tag{3.13}$$

Finally, the second integral in (3.11) can be simplified in the following way:

$$\sum_{i=1}^{m} \int_0^L \alpha_i^p (\bar{N}_i)^T u_i^p(x_1)\,\mathrm{d}x_1 = \sum_{i=1}^{m} \alpha_i^p (\bar{N}_i)^T \int_0^L u_i^p(x_1)\,\mathrm{d}x_1$$
$$= \sum_{i=1}^{m} \alpha_i^p (\bar{N}_i)^T \int_0^L T_i^T y_i^p(x_1)\,\mathrm{d}x_1 =: \sum_{i=1}^{m} \alpha_i^p c_{p,i} =: c_p(\alpha). \tag{3.14}$$

Note that $u_i^p(x_1)$ does not depend on the state at each node of beam i and therefore can be recalculated by analytically solving the beam problem (2.17). We can explicitly state for beam i:

$$c_{p,i} = \frac{1}{12}(\bar{N}_{i1})^2 \frac{L^3}{EA} + \frac{1}{720}(\bar{N}_{i2})^2 \frac{L^3(kGA\,L^2 + 60EI)}{kGA\,EI} + \frac{1}{720}(\bar{N}_{i3})^2 \frac{L^3(kGA\,L^2 + 60EI)}{kGA\,EI}. \tag{3.15}$$

Summing up, we obtain the following representation of the compliance functional:

$$c(\alpha, y(\alpha)) := c_1(\alpha, y(\alpha)) + c_2(\alpha, y(\alpha)) + c_p(\alpha)$$
$$= (\hat{f}^{\mathrm{nod}})^T y(\alpha) + \sum_{i=1}^{m} \alpha_i^p (\hat{f}_i^{\mathrm{dist}})^T y(\alpha) + c_p(\alpha) = f(\alpha)^T y(\alpha) + c_p(\alpha), \tag{3.16}$$

where we again used $f = \hat{f}^{\mathrm{nod}} + \sum_{i=1}^{m} \alpha_i^p \hat{f}_i^{\mathrm{dist}}$. Now we can formulate the topology-optimization problem:

$$\begin{aligned} \min_{\alpha \in \mathbb{R}^m} \quad & c(\alpha, y(\alpha)) = f(\alpha)^T y(\alpha) + c_p(\alpha) \\ \text{s.t.} \quad & \left(\sum_i^m \alpha_i^p \hat{K}_i^{\mathrm{loc}}(x) \right) y(\alpha) = \hat{f}^{\mathrm{nod}} + \sum_i^m \alpha_i^p \hat{f}_i^{\mathrm{dist}} \\ & \sum_i^m \alpha_i V_i \le V \\ & 0 < \alpha_{\min} \le \alpha_i \le 1, \quad \forall i. \end{aligned} \tag{3.17}$$

If we want to solve optimization problem (3.17), are confronted with the difficulty that our problem is nonconvex. As a consequence, starting out directly with a high penalty parameter p we may become trapped in an undesired local minimum. To weaken this effect, a continuation strategy similar to [13] is applied in this work. In Section 4 we will present results computed by the SQP code SNOPT (see [10]). In order to be able to solve (3.17) using SNOPT in a quick and robust way, the gradient of the objective function is required. The gradient of the term $f(\alpha)^T y(\alpha)$ can be calculated via standard adjoint calculus. The gradient of the term $c_p(\alpha)$ is straightforward, as $c_{p,i}$ in (3.14) is design-independent. The gradient reads as follows:

$$\frac{\partial c}{\partial \alpha_i} = p\,\alpha_i^{p-1}(-y^T \hat{K}_i^{\mathrm{loc}} y + 2(\hat{f}_i^{\mathrm{dist}})^T y) + p\,\alpha_i^{p-1} c_{p,i}, \; i = 1, 2, \ldots, m. \tag{3.18}$$

3.2. Simultaneous material and topology optimization using the DMO-approach

In the previous section, the same material parameters were used for all beams in the network. However in the final topology optimization result, there are still some beams which are more important for load transmission, and some which are less important. This observation motivated us to also investigate a multi-material optimization model.

Again we consider a 3-D beam network geometry, but we now have m_c predefined materials from a catalogue for each of the m design objects (beams). Using this, the material optimization problem reads as follows: assign

exactly one material (or a void material) to every beam, such that a given objective function (*e.g.* compliance) is minimized. In this form, the posed problem is a combinatorial optimization problem, which cannot be solved in reasonable time for larger networks. Fortunately, an approximation using continuous variables is possible, adopting ideas of [12,13,19,28,29]. This concept is called Discrete Material Optimization (DMO) and is applied to Timoshenko beams networks in the subsequent section.

The design parametrization is slightly different from the parametrization presented in Section 3.1. As there exist m_c design variables for every beam, hence we obtain two indices on the design variable $\alpha_{ij} \in [0,1],\ i = 1,2,\dots,m_c,\ j = 1,2,\dots,m$ with the following meaning:

$$\alpha_{ij} = \begin{cases} 1 & \text{if material } i \text{ is chosen on beam } j \text{ in current geometry,} \\ \alpha_{\min} > 0 & \text{if not.} \end{cases} \tag{3.19}$$

The total number of design variables amounts to $m_c m$. Thus, the material optimization problem in the continuous form reads as follows:

$$\begin{aligned} \min_{\alpha \in \mathbb{R}^{m_c \times m}} \quad & c(\alpha, y(\alpha)) = f(\alpha)^T y(\alpha) + c_p(\alpha) \\ \text{s.t.} \quad & K(\alpha) y(\alpha) = f(\alpha) \\ & \sum_{i=1}^{m_c} \sum_{j=1}^{m} \alpha_{ij} \rho_j V_j \le M \\ & \sum_{i=1}^{m_c} \alpha_{ij} = 1, \quad \forall j \\ & \alpha_{ij} \ge \alpha_{\min} > 0, \quad \forall i, j. \end{aligned} \tag{3.20}$$

Note that the design variables in the volume constraint are now weighted with a factor, in this case the density ρ_j of the material j. To assemble the global stiffness matrix K, an interpolation between local stiffness matrices of all materials is utilized. In order to get approximately discrete solutions, a penalization approach similar to the SIMP scheme is used. Now the new interpolation rule can be formulated (following [13]) as

$$K(\alpha) = \sum_{i=1}^{m_c} \sum_{j=1}^{m} \alpha_{ij}^p \hat{K}_{ij}^{\text{loc}}(\alpha), \qquad p > 1. \tag{3.21}$$

The penalization combined with the resource constraint in (3.20) makes material-mixtures unattractive with regard to the objective function and again pushes the optimizer towards a discrete solution. The constraint

$$\sum_{i=1}^{m_c} \alpha_{ij} = 1, \quad \forall j \tag{3.22}$$

in conjunction with the box constraint $\alpha_{ij} \ge \alpha_{\min}$ guarantees that exactly one material is chosen per beam. If a void material is contained in the catalogue of possible materials, a simultaneous topology- and multi-material optimization is obtained. Similar to the previous section, a continuation strategy is applied during optimization. Again, it will be demonstrated in Section 4 that problem (3.20) can be solved with SNOPT. Using the same techniques described in Section 3.1, we obtain the following formula for the gradient of the objective function, which now has length $m_c\, m$:

$$\begin{aligned} & \frac{\partial c}{\partial \alpha_{ij}} = p\, \alpha_{ij}^{p-1} (-y^T \hat{K}_{ij}^{\text{loc}} y + 2(\hat{f}_{ij}^{\text{dist}})^T y) + p\, \alpha_{ij}^{p-1} c_{p,ij}, \\ & i = 1,\dots,m_c,\ j = 1,\dots,m. \end{aligned} \tag{3.23}$$

The partial derivatives of the resource and combinatorial constraint are straightforward, as both linearly depend on the design α_{ij}.

4. Numerical examples

As a prerequisite for this section, the solution of the 3D Timoshenko beam network problem described in Section 2 has been implemented as MATLAB code and interfaced to the SQP code SNOPT, which is utilized to solve the optimization problems (3.17) and (3.20).

Before we go into the details of the examples we would like to mention that the goal of this section is to demonstrate the efficiency of our approach when applied in the framework of typical structural optimization problems. For this, we restrict ourselves to stiffness-*vs.*-weight optimization rather than including additional constraints, *e.g.* on stresses. The chosen material parameters do not always fully correspond to real materials as, for instance, steel grades but are altered in such a way that the optimization result gets more interesting in the sense that each of the different material is chosen in several places of the optimized design. Moreover, we recall that all state problem are fully linear, *i.e.* a linear constitutive law is used and displacements are assumed to be small.

4.1. Numerical study for ansatz-functions

In Section 2.2 we proved that our simulation approach yields analytic solutions to the beam network problem at every node, while only one shape function per beam is used and no refinement is necessary. These properties are crucial for optimization, especially for our topology and multi-material optimization with a large number of potential bars (for example generated by the well-known ground structure approach, [6]).

In addition to the theoretical result in Section 2.2, in this subsection we wish to present a numerical study of the performance of our ansatz-functions in comparison to linear ansatz-functions with and without shear locking correction. For the latter we have implemented the reduced integration approach according to [23].

Consider a single-load cantilever structure of length 24 m with two fixed points D_1 and D_2 as illustrated in Figure 2. The structure is loaded with self-weight due to gravity as well as a fixed nodal force f_N at node F and consists of beams with material properties displayed in Table 2. The structure is simulated with analytic and linear ansatz-functions (with and without reduced integration) and varying global refinements (see Tab. 1). The compliance as defined in Section 3 and the displacement in the y-direction at node F is monitored. Global refinement of factor n means that one initial beam is split up into n beams, consequently factor 1 means no refinement. The table reveals, that shear locking occurs for linear ansatz-functions with coarse refinements, and thus the displacement at node F is underestimated. Further refinements lead to a numerical convergence of both compliance and displacement at node F to the values obtained by our analytic shape functions with no refinement. Many global refinement steps are required for a small discretization error. A similar observation is made for the computations with under integration: although the underestimation of the stiffness at the end node F disappears, still a lot of global refinements are required to reach the desired precision. Clearly, the calculation time to solve $Ky = f$ increases with the refinement factor. On the computer used for this simulation the solution with analytic shape functions and no refinement was calculated 5×10^3 times faster that the solution with linear shape functions and refinement factor 10 000. Of course, more advanced beam elements could be used; it is noted

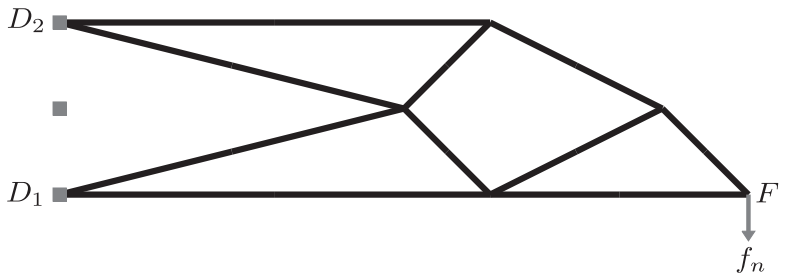

Figure 2. Cantilever beam.

TABLE 1. Shape functions with varying refinements.

Shape functions	Global refinement	Compliance $c(y)$	Displacement y_F [m]
Analytic	1	2138.26	−0.0102667
Linear	2	1422.63	−0.0084092
	10	1856.76	−0.0101416
	100	2126.91	−0.0102652
	1000	2138.14	−0.0102666
	10000	2138.26	−0.0102667
Linear (with reduced integration, see [23])	2	1864.53	−0.0103422
	10	2123.83	−0.0102696
	100	2138.11	−0.0102667
	1000	2138.26	−0.0102667

TABLE 2. Material properties.

Material parameter		Value
Mass density	ρ	$7840\,\mathrm{kg\,m^{-3}}$
Poisson's ratio	ν	0.3
Elastic modulus	E	$1.7 \times 10^{11}\,\mathrm{N\,m^{-2}}$
Shear modulus	G	$6.54 \times 10^{10}\,\mathrm{N\,m^{-2}}$
Cross-sectional area	A	$0.02545\,\mathrm{m^2}$
Second area moments	I_2	$2.347 \times 10^{-4}\,\mathrm{m^4}$
	I_3	$2.347 \times 10^{-4}\,\mathrm{m^4}$
	I_t	$4.695 \times 10^{-4}\,\mathrm{m^4}$
Shear correction factor	k	0.541

however that (after precomputing local stiffness matrices, which is possible, *e.g.* for the optimization examples discussed below) an assembly and solution step with the analytic approach is not more expensive than the same operation using linear ansatz functions.

4.2. 3D-bridge

In this example we simulate a 3D bridge structure under constant nodal forces and self-weight (see Fig. 3a). The domain has a size of $32\,\mathrm{m} \times 16\,\mathrm{m} \times 12\,\mathrm{m}$ and consists of 180 nodes and 13369 potential beams. The structure has two fixed bearings on the left and two sliding bearings on the right. The structure is loaded with constant forces $f = -1 \times 10^6$ N on all nodes denoted in Figure 3a and self-weight due to gravity. All potential elements are steel beams with material properties as defined in Table 2. The minimal compliance solution for the topology optimization problem (3.17) with volume $V = 15.7\,\mathrm{m}^3$, which is roughly 0.27% of the entire potential volume, is shown in Figure 3b and c (undeformed geometry). Table 5 summarizes important figures for this example, in particular the mass, the compliance value and the number of userfunction calls (evaluation of the state problem and the derivatives) during optimization.

We conclude this study with a brief comparison of topology optimization for beam and truss models. We recomputed the bridge example using a truss model. The result revealed that the best topologies found for the truss model and the beam network model were precisely the same. Thus, in this particular example – if one is only interested in the optimal topology and not in the precise deformation states – one could have opted for a numerically cheaper truss model from the very beginning. On the other hand it turns out that – thanks to the analytic approach we were using – there is only little computational overhead, when using the physically

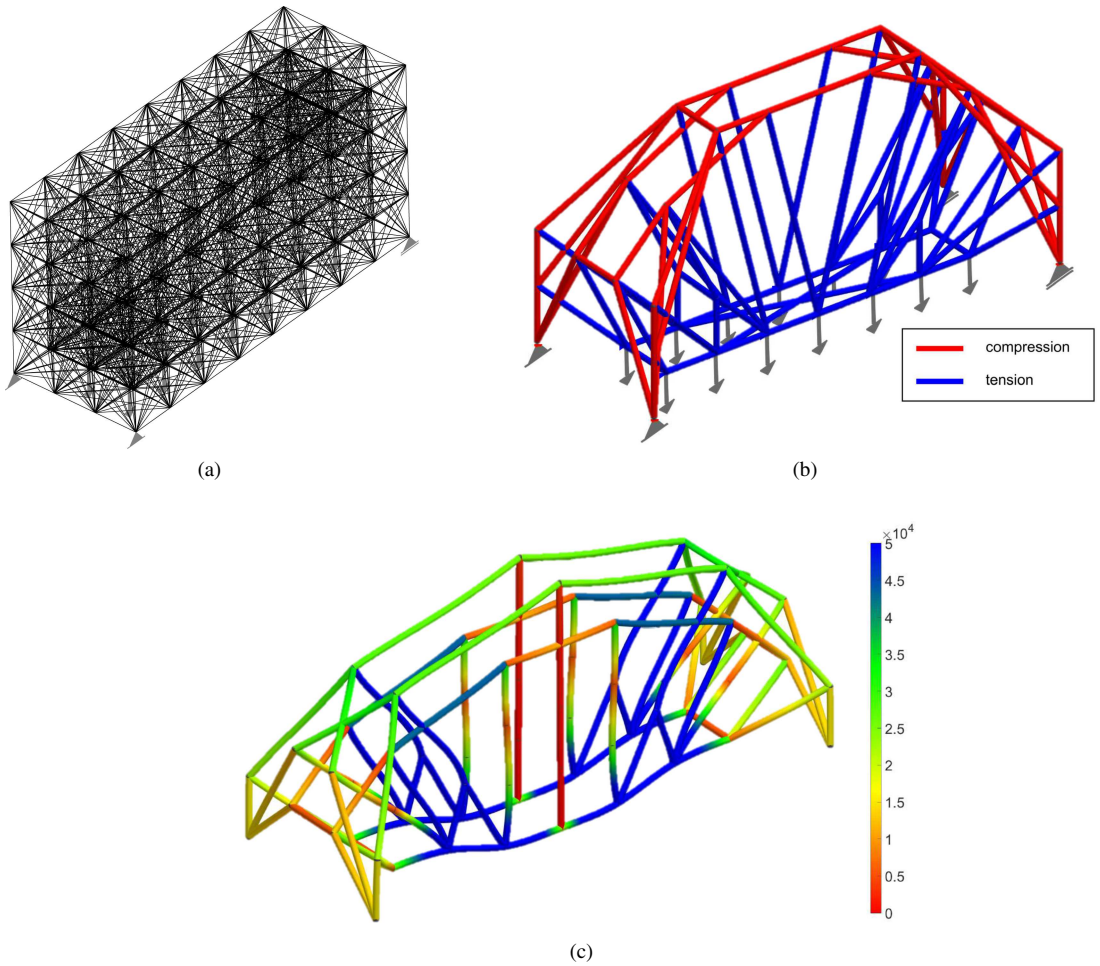

(a) (b)

(c)

FIGURE 3. Topology optimization (3D-Bridge): (a) ground structure with boundary conditions (b) topology solution (3D view, coloring: normal forces) (c) deformed topology solution (3D view, coloring: normed bending moments).

more correct beam model instead of a truss. Indeed Table 3 shows that, if the same optimization formulation and algorithm is applied, approximately the same number of iterations are required. In each iteration, the state problem has to be assembled, solved and gradients have to be computed. While the required time for the sensitivity analysis is approximately the same, the computation times for assembling and system solution differ by approximately a factor 2–3. This is in perfect analogy with the different number of entries in the local and global stiffness matrix for the truss and the beam model, respectively. Taking also the overhead of the optimizer itself into account, the resulting total time for the beam network optimization is less than 35% more expensive than the truss approach. This seems to be a rather low price for the more exact solution.

4.3. 3D-bridge multi-material

This example uses the same 3D bridge geometry with identical loads and boundary conditions as the first numerical example (see Fig. 3a). In this case, however, we allow the optimizer to choose from three different materials (and an additional void material). The candidate materials differ in the following properties: elastic

TABLE 3. Computational statistics: comparison to a truss topology design approach.

	# user functions	Total time [s]	Avg. time [s] for state problem assembling	Avg. time [s] for state problem solution	Avg. time [s] for sensitivity analysis
Beam network	501	310	0.280	0.048	0.055
Truss	543	230	0.122	0.013	0.056

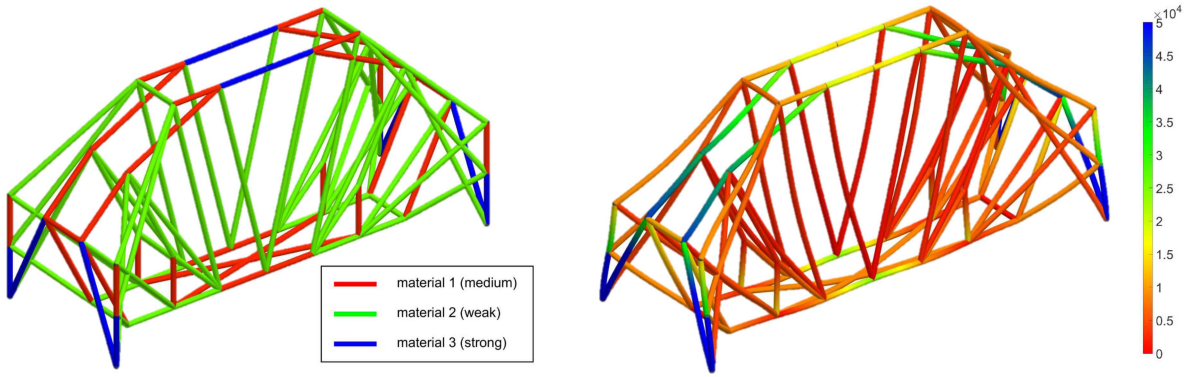

(a) (b)

FIGURE 4. Multi-material optimization (3D-Bridge), $M = 1.17 \times 10^5$ kg; (a): material selection; (b): deformed Topology solution (3D view, coloring: normed bending moments).

TABLE 4. Multi-material properties.

Material parameter		Material 1	Material 2	Material 3
Cross-sectional area	A	$0.02545\ \mathrm{m}^2$	$0.01131\ \mathrm{m}^2$	$0.04524\ \mathrm{m}^2$
Second area moments	I_2	$2.347 \times 10^{-4}\ \mathrm{m}^4$	$4.637 \times 10^{-5}\ \mathrm{m}^4$	$7.419 \times 10^{-4}\ \mathrm{m}^4$
	I_3	$2.347 \times 10^{-4}\ \mathrm{m}^4$	$4.637 \times 10^{-5}\ \mathrm{m}^4$	$7.419 \times 10^{-4}\ \mathrm{m}^4$
	I_t	$4.695 \times 10^{-4}\ \mathrm{m}^4$	$9.274 \times 10^{-5}\ \mathrm{m}^4$	$1.484 \times 10^{-3}\ \mathrm{m}^4$
Shear correction factor	k	0.541	0.541	0.541
Elastic modulus	E	$1.7 \times 10^{11}\ \mathrm{N\,m}^{-2}$	$1.78 \times 10^{11}\ \mathrm{N\,m}^{-2}$	$1.7 \times 10^{11}\ \mathrm{N\,m}^{-2}$
Shear modulus	G	$6.54 \times 10^{10}\ \mathrm{N\,m}^{-2}$	$6.54 \times 10^{10}\ \mathrm{N\,m}^{-2}$	$6.84 \times 10^{10}\ \mathrm{N\,m}^{-2}$
Poisson's ratio	ν	0.3	0.36	0.24
Mass density	ρ	$7840\ \mathrm{kg}$	$8040\ \mathrm{kg}$	$8240\ \mathrm{kg}$
Mass per length	ρA	$199.5\ \mathrm{kg\,m}^{-1}$	$90.9\ \mathrm{kg\,m}^{-1}$	$372.8\ \mathrm{kg\,m}^{-1}$

modulus, shear modulus, Poisson's ratio, cross-sectional area, moments of area, mass density and thus mass per length. The material parameters for the three candidate materials are shown in Table 4. Material 1 is precisely the material used in the topology optimization example and will be referred to as "medium material". In comparison, material 2 has a lower cross-sectional area and a slightly higher elastic modulus, which results in lower shear, bending and axial stiffness. We thus call this material "weak material". Material 3 has a large cross-sectional area and moreover a higher shear modulus, which results in higher stiffness, especially shear stiffness. However, it also has higher costs in terms of resource consumption and a higher self-weight. We call this material "strong material".

Figure 4a depicts a solution of the multi-material optimization problem (3.20) with mass $M = 1.17 \times 10^5$ kg. The compliance value and the number of userfunction calls during optimization can be found in Table 5. To

TABLE 5. Comparison of examples.

3D-Bridge	$c(\alpha, y(\alpha))$ [Nm]	mass M [kg]	# userfunction
Topology optimization	20.365	1.197×10^5	501
Multi-material optimization	17.645	1.172×10^5	541

TABLE 6. Material catalogue of pipes for the bicycle problem.

Pipe	Outer diameter/ width [mm]	Wall thickness [mm]	Shape of cross section
mat 1	25.4	0.7	Circular
mat 2	25.4	1.0	Circular
mat 3	38.1	0.7	Circular
mat 4	38.1	1.0	Circular
mat 5	13.45	0.7	Rectangular
mat 6	13.45	1.0	Rectangular
mat 7	19.05	0.7	Rectangular
mat 8	19.05	1.0	Rectangular

conclude this numerical example, we provide a short analysis. The solution of the topology optimization problem (3.17) is part of the admissible set for the multi-material optimization problem (3.20) if we assume a similar resource constraint. Therefore, we expect the solution of the latter problem to be equally good or better in terms of the objective function. As we can see in Figure 4a, strong material is used for highly stressed beams near the bearings and in the middle of the bridge, whereas weak material is used for less exposed beams. As a result, a significantly better compliance with a similar (or slightly lower) resource constraint is achieved (see Tab. 5).

4.4. A multi-material bicycle frame

As we have seen in the previous examples, optimization obtained using our analytic beam network approach may in certain cases hardly differ from results obtained by truss topology design. This is in particular expected for very dense and regular ground structures as in this case bending in the members becomes less prominent for an optimal structure. On the other hand there exist examples, for which the ground structure is naturally sparse. A prominent example falling into this category is the frame of a car [36, 37] or a bicycle as discussed in this section, see Figure 5. The frame we consider is loaded by vertical forces acting simultaneously on the saddle, at both ends of the handle bar as well as the position where the pedals are mounted. Moreover the frame is supported at the front and the back wheel hub. At the front wheel hub displacements are completely fixed, while at the rear hub displacement is fixed only in one direction; no constraints on moments are applied in both places.While we assume that the topology of the frame is fixed, we search for an optimal combination of aluminium pipes with different cross sectional shapes. We perform two studies: we first solve the design problem with only circular pipes of different outer diameters and wall thicknesses (materials 1–4 in Tab. 6) and then, in a second step, add pipes with a rectangular cross section exhibiting an aspect ratio of 1 for the width to 2 for the height (materials 5–8 in Tab. 6). As there are only 20 nodes and 22 beams in the frame model and, thanks to the analytic approach, no refinement is necessary, we can solve both DMO problems repeatedly with 1000 random starts in a few minutes (computation times for an individual instance range between 0.2 and 0.5 seconds; on the average 47 iterations are required for the example with 4 materials and 55 for the example with 8 materials).

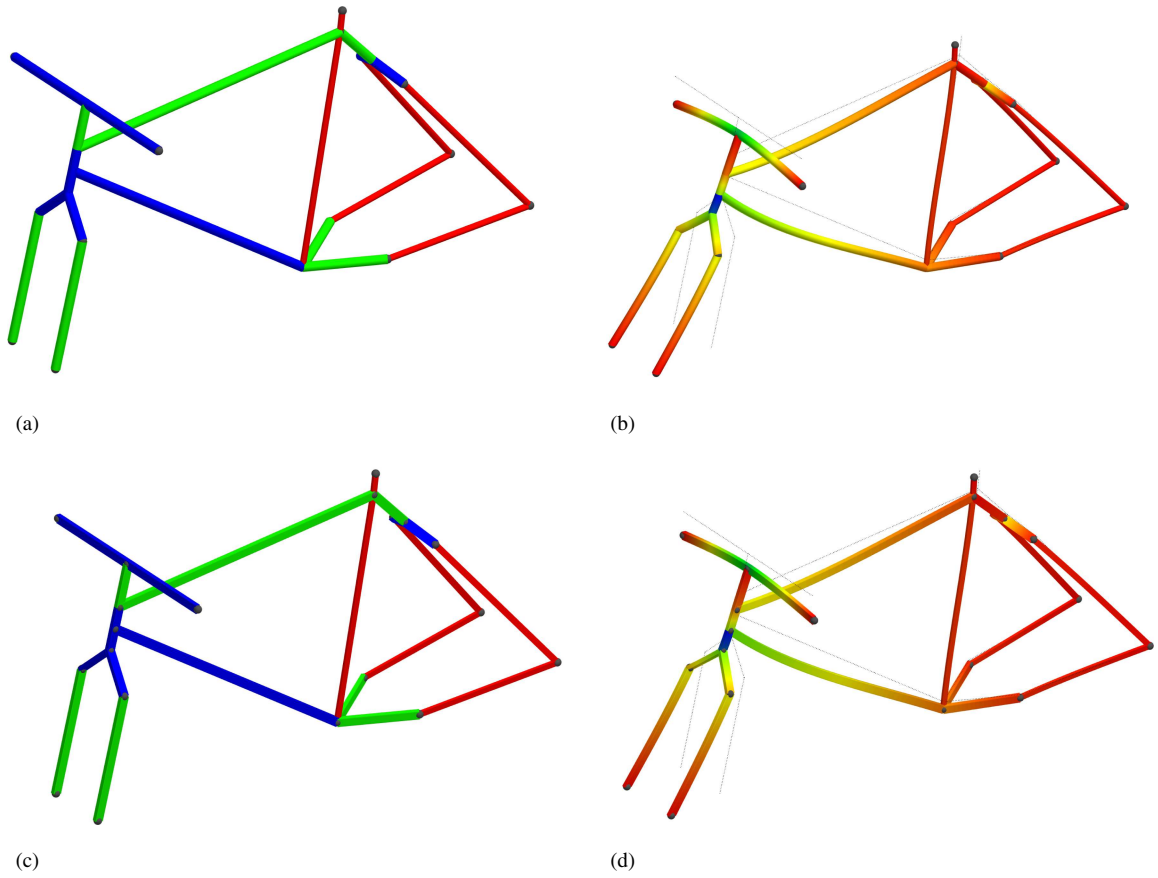

FIGURE 5. Multi-material optimization of a bicycle frame; (a) shows the result, if only circular pipes are allowed – the total weight is 1.259 kg; only mat 1 (red), mat 3 (green) and mat 4 (blue) are used. ((b) visualizes the deformation of the frame as well as the total bending moment; in (c) the solution is displayed if also rectangular cross sections are allowed – obviously only rectangular pipes (red=mat 5, green=mat 7, blue=mat 8) are selected; (d) displays deformation and bending again.

The results are displayed in Figure 5. If only circular pipes are allowed, the total weight obtained is 1.259 kg; if also rectangular cross sections are allowed, the weight decreases slightly to 1.247 kg, however the compliance is better by about 17%. Again looking at Figure 5, it becomes clear that only rectangular cross sections are used in that case.

5. Conclusions and future research

In this article, we derived a 3D-Timoshenko beam network modelassuming small displacements and linear constitutive laws. Furthermore, we obtained an efficient FE-type numerical scheme to calculate analytic solutions for the network problem.

With this as a basis, we formulated topology and multi-material optimization problems. These nonlinear optimization problems could be solved by a SQP-method. The so-called analytic shape functions proved to be particularly useful for optimization as they enable the frequent numerical evaluation of the state problem to be performed in a fast and accurate manner. Therefore, with respect to computational complexity, our

optimization results for a 3D-Timoshenko beam network can be calculated to the same order of magnitude as for truss optimization. Finally, we presented results based on our MATLAB implementation using the SNOPT software.

In future, it may be interesting to formulate and investigate sizing as well as shape optimization models based on the linear Timoshenko beam network theory presented in this article.

Acknowledgements. The authors would like to acknowledge the generous support of the Deutsche Forschungsgemeinschaft, Grant number DFG CRC 814 (Project C2).

References

[1] W. Achtziger, M.P. Bendsøe, A. Ben-Tal and J. Zowe, Equivalent displacement based formulations for maximum strength truss topology design. *IMPACT Comput. Sci. Eng.* **4** (1992) 315–345.

[2] A. Ben-Tal and M.P. Bendsøe, A new method for optimal truss topology design. *SIAM J. Optim.* **3** (1993) 322–358.

[3] M.P. Bendsøe, Optimal shape design as a material distribution problem. *Struct. Optim.* **1** (1989) 192–202.

[4] M.P. Bendsøe, A. Ben-Tal and J. Zowe, Optimization methods for truss geometry and topology design. *Struct. Multi. Optim.* **7** (1994) 141–159.

[5] R. Davis, R.D. Henshell and G.B. Warburton, A Timoshenko beam element. *J. Sound Vibr.* **22** (1972) 475–487.

[6] W.S. Dorn, R.E. Gomory and H.J. Greenberg, Automatic design of optimal structures. *J. Mech.* **3** (1964) 25–52.

[7] H. Fredricson, Topology optimization of frame structures-joint penalty and material selection. *Struct. Multi. Optim.* **30** (2005) 193–200.

[8] H. Fredricson, T. Johansen, A. Klarbring and J. Petersson, Topology optimization of frame structures with flexible joints. *Struct. Multi. Optim.* **25** (2003) 199–214.

[9] Z. Friedman and J.B. Kosmatka, An improved two-node timoshenko beam finite element. *Comput. Struct.* **47** (1993) 473–481.

[10] P.E. Gill, W. Murray and M.A. Saunders, SNOPT: an SQP algorithm for large-scale constrained optimization. *SIAM J. Optim.* **12** (2002) 979–1006.

[11] W.S. Hemp, Optimum Structures. Clarendon Press Oxford, Oxford (1973).

[12] C. Hvejsel, E. Lund and M. Stolpe, Optimization strategies for discrete multi-material stiffness optimization. *Struct. Multi. Optim.* **44** (2011) 149–163.

[13] C.F. Hvejsel and E. Lund, Material interpolation schemes for unified topology and multi-material optimization. *Struct. Multi. Optim.* **43** (2011) 811–825.

[14] G. Jelenić and E. Papa, Exact solution of 3D Timoshenko beam problem using linked interpolation of arbitrary order. *Arch. Appl. Mech.* **81** (2011) 171–183.

[15] K. Kapur, Vibrations of a Timoshenko beam using finite-element approach. *J. Acoust. Soc. Am.* **40** (1966) 1058–1063.

[16] M. Kočvara, Topology optimization with displacement constraints: a bilevel programming approach. *Struct. Optim.* **14** (1997) 256–263.

[17] J.E. Lagnese and E.J.P.G. Leugering and G. Schmidt, Modeling, Analysis and Control of Dynamic Elastic Multi-link Structures. Birkhäuser Boston Inc., Boston, MA (1994).

[18] A.W. Lees and D.L. Thomas, Unified Timoshenko beam finite element. *J. Sound Vibr.* **80** (1982) 355–366.

[19] E. Lund and J. Stegmann, On structural optimization of composite shell structures using a discrete constitutive parametrization. *Wind Energy* **8** (2005) 109–124.

[20] Y. Luo, An efficient 3D timoshenko beam element with consistent shape functions. *Adv. Theor. Appl. Mech.* **1** (2008) 95–106.

[21] S. Mukherjee and G. Prathap, Analysis of shear locking in Timoshenko beam elements using the function space approach. *Commun. Numer. Methods Eng.* **17** (2001) 385–393.

[22] E. Papa Dukić and G. Jelenić, Exact solution of 3D Timoshenko beam problem: problem-dependent formulation. *Arch. Appl. Mech.* **84** (2014) 375–384.

[23] G. Prathap and G.R. Bhashyam, Reduced integration and the shear-flexible beam element. *Int. J. Numer. Methods Eng.* **18** (1982) 195–210.

[24] J.N. Reddy, On locking-free beam finite elements. *Comput. Methods Appl. Mech. Eng.* **7825** (1997) 113–132.

[25] I. Romero and F. Armero, An objective finite element approximation of the kinematics of geometrically exact rods and its use in the formulation of an energymomentum conserving scheme in dynamics. *Int. J. Numer. Methods Eng.* **54** (2002) 1683–1716.

[26] G.I.N. Rozvany, T. Lewiński and M. Zhou, Extended exact solutions for least-weight truss layouts-Part I: cantilever with a horizontal axis of symmetry. *Int. J. Mech. Sci.* **36** (1994) 375–398.

[27] I. Senjanović, N. Vladimir and D.S. Cho, A shear locking-free beam finite element based on the modified Timoshenko beam theory. *Trans. FAMENA* **37** (2013) 1–16.

[28] J. Stegmann, *Analysis and optimization of laminated composite shell structures*. Ph.D. thesis (2004).

[29] J. Stegmann and E. Lund, Discrete material optimization of general composite shell structures. *Int. J. Numer. Methods Eng.* **62** (2005) 2009–2027.

[30] R.L. Taylor, F.C. Filippou, A. Saritas, and F. Auricchio, A mixed finite element method for beam and frame problems. *Comput. Mech.* **31** (2003) 192–203.
[31] A. Tessler and S.B. Dong, On a hierarchy of conforming timoshenko beam elements. *Comput. Struct.* **14** (1981) 335–344.
[32] D.L. Thomas, J.M. Wilson and R.R. Wilson, Timoshenko beam finite elements. *J. Sound Vibr.* **31** (1973) 315–330.
[33] J. Thomas and B.A.H. Abbas, Finite element model for dynamic analysis of Timoshenko beam. *J. Sound Vibr.* **41** (1975) 291–299.
[34] S.P. Timoshenko, On the correction for shear of the differential equation for transverse vibrations of prismatic bars. *Philos. Mag.* **41** (1921) 744–746.
[35] S.P. Timoshenko, On the transverse vibrations of bars of uniform cross-section. *Philos. Mag.* **43** (1922) 125–131.
[36] B. Torstenfelt and A. Klarbring. Structural optimization of modular product families with application to car space frame structures. *Struct. Multi. Optim.* **32** (2006) 133–140.
[37] B. Torstenfelt and A. Klarbring, Conceptual optimal design of modular car product families using simultaneous size, shape and topology optimization. *Finite Ele. Anal. Des.* **43** (2007) 1050–1061.
[38] T. Yokoyama, A reduced integration Timoshenko beam element. *J. Sound Vibr.* **169** (1994) 411–418.